Radical−Copper Wheels: Structure and Magnetism of Hexanuclear Hybrid Arrays

Junichi Omata, Takayuki Ishida,*,† Daisuke Hashizume, Fujiko Iwasaki, and Takashi Nogami*

Department of Applied Physics and Chemistry, The University of Electro-Communications, Chofu, Tokyo 182-8585, Japan

Received December 27, 2000

Complexation of copper(II) bromide and chloride with 4-pyrimidinyl nitronyl nitroxide (4PMNN) as a bridging ligand gave discrete hexanuclear complexes carrying 12 spins, $[CuX_2\cdot(4PMNN)]_6$ [X = Br (**1**), Cl (**2**)], which crystallize in a trigonal space group $R\bar{3}$. The crystallographic parameters are $C_{11}H_{15}Br_2CuN_4O_2\cdot 0.3H_2O$, a = 28.172(2), c = 12.590(2) Å, V = 8653(2) Å^3, and Z = 18 for **1**, and $C_{11}H_{15}Cl_2CuN_4O_2\cdot 0.3H_2O$, a = 28.261(2), c = 12.378(1) Å, and Z = 18 for **2**. The hexanuclear arrays construct a perfect column perpendicular to the molecular plane. The diameter of the resultant honeycomblike channel is ca. 11.5 Å defined by the interatomic distance of two opposing copper ions. Their magnetic behavior is interpreted as the simultaneous presence of ferro and antiferromagnetic couplings. The ferromagnetic couplings are attributed to the interactions between a copper spin and the axially coordinated nitronyl nitroxide spin and between nitronyl nitroxide groups through van der Waals contacts. The antiferromagnetic coupling is due to the interaction between copper ions across the pyrimidine bridges.

Introduction

The metal−radical approach has been successful in the design of ferrimagnetic compounds that show magnetic order at low temperatures.[1,2] The synthesis and magnetic property of a hexanuclear compound containing six *cis*-Mn(hfac)$_2$ entities connected by phenyl nitronyl nitroxide have been reported.[3] Self-assembled oligonuclear complexes sometimes possess architectural beauty.[4−6] Such polynuclear discrete molecules have fascinated chemists owing especially to their mesoscopic physical properties (magnetic hysteresis of purely molecular origin, for instance).[7,8] We have reported the magnetism of pyrimidine-bridged transition metal complexes[9−12] in connection with the organic high-spin *m*-phenylene-bridged polycarbenes and radicals.[13] In the course of our study on the magnetic role of radical-substituted pyrimidine across μ-1,3-NCN bridges, we have found that hexanuclear arrays $[CuX_2\cdot(4PMNN)]_6$ (**1**: X = Br, **2**: X = Cl; 4PMNN = 4-pyrimidinyl nitronyl nitroxide[14]) exhibited ferromagnetic intermolecular interactions.

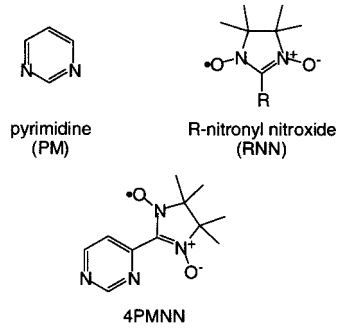

Experimental Section

The 4-pyrimidinecarboxaldehyde was prepared according to the method previously reported,[15] by using *N*,*N*-dimethylformamide diethyl acetal and pyruvic aldehyde dimethyl acetal as starting materials. The formyl group was converted to a nitronyl nitroxide group by Ullman's method,[16] giving blue plates of 4PMNN in 76% yield from 4-pyrimidinecarboxaldehyde (mp 128−131 °C, recrystallized from ether−hexane). Anal. Calcd for $C_{11}H_{15}N_4O_2$: C, 56.16; H, 6.43; N, 23.82%. Found: C, 56.64; H, 6.48; N, 23.63%. MS (EI, 70 eV) *m*/*z* 236 (68%, MH^+), 106 (100%). ESR (benzene, room temperature) g = 2.0065, a_N = 7.1 G (quintet).

The typical procedure of complexation is as follows. A methanol solution (10 mL) containing 34 mg (0.14 mmol) of 4PMNN and 35 mg (0.16 mmol) of $CuBr_2$ was allowed to stand at room temperature for a week. Dark green needles (18 mg, 0.039 mmol) of **1** were precipitated and collected on a filter; the crystals were suitable for X-ray

* To whom communication should be addressed.
† E-mail: ishi@pc.uec.ac.jp.

(1) Caneschi, A.; Gatteschi, D.; Rey, P.; Sessoli, R. *Acc. Chem. Res.* **1989**, *22*, 392.
(2) Inoue, K.; Hayamizu, T.; Iwamura, H.; Hashizume, D.; Ohashi, Y. *J. Am. Chem. Soc.* **1996**, *118*, 1803.
(3) Caneschi, A.; Gatteschi, D.; Laugier, J.; Rey, P.; Sessoli, R.; Zanchini, C. *J. Am. Chem. Soc.* **1988**, *110*, 2795.
(4) Taft, K. L.; Lippard, S. J., *J. Am. Chem. Soc.* **1990**, *112*, 9629.
(5) Abbati, G. L.; Cornia, A.; Fabretti, A. C.; Caneschi, A.; Gatteschi, D. *Inorg. Chem.* **1998**, *37*, 1430.
(6) Blake, A. J.; Grant, C. M.; Parsons, S.; Rawson, J. M.; Winpenny, E. P. *J. Chem. Soc., Chem. Commun.* **1994**, 2363.
(7) Friedman, J. R.; Sarachik, M. P.; Tejada, J.; Ziolo, R. *Phys. Rev. Lett.* **1996**, *76*, 3830.
(8) Thomas, L.; Lionti, F.; Ballow, R.; Gatteschi, D.; Sessoli, R.; Barbara, B. *Natrure* **1996**, *383*, 145.
(9) Ishida, T.; Nogami, T. *Recent Res. Devel. Pure Appl. Chem.* **1997**, *1*, 1.
(10) Ishida, T.; Nakayama, K.; Nakagawa, M.; Sato, W.; Ishikawa, Y.; Yasui, M.; Iwasaki, F.; Nogami, T. *Synth. Met.* **1997**, *85*, 1655.
(11) Nakayama, K.; Ishida, T.; Takayama, R.; Hashizume, D.; Yasui, M.; Iwasaki, F.; Nogami, T. *Chem. Lett.* **1998**, 497.
(12) Kusaka, T.; Ishida, T.; Hashizume, D.; Iwasaki, F.; Nogami, T. *Chem. Lett.* **2000**, 1146.
(13) Iwamura, H. *Adv. Phys. Org. Chem.* **1990**, *26*, 179.
(14) Systematic name: 2-(4-pyrimidinyl)-4,4,5,5-tetramethylimidazolin-1-yloxyl 3-oxide.
(15) Bredereck, H.; Sell, R.; Effenberger, F. *Chem. Ber.* **1964**, *97*, 3406.
(16) Ullman, E. F.; Osiecki, J. H.; Darcy, R. *J. Am. Chem. Soc.* **1972**, *94*, 7049.

10.1021/ic001462g CCC: $20.00
Published on Web 06/27/2001

Table 1. Crystallographic Data of **1** and **2**

formula	$C_{11}H_{15}Br_2CuN_4O_2\cdot0.3H_2O$	$C_{11}H_{15}Cl_2CuN_4O_2\cdot0.3H_2O$
fw	464.02	375.12
space group	$R\bar{3}$	$R\bar{3}$
a/Å	28.172(2)	28.261(2)
c/Å	12.590(2)	12.378(1)
V/Å^3	8653(2)	8561(1)
Z	18	18
D_{calc}/g cm^{-3}	1.605	1.312
μ(Mo Kα)/mm^{-1}	5.298	1.435
R^a ($I > 2\sigma(I)$)	0.0576	0.0605
$R_w{}^b$ ($I > 2\sigma(I)$)	0.102	0.118
T/K	296	296
λ/Å	0.71073	0.71073

[a] $R = \sum||F_o| - |F_c||/\sum|F_o|$. [b] $R_w = [\sum w(F_o^2 - F_c^2)^2/\sum w(F_c^2)^2]^{1/2}$.

diffraction and magnetic studies. Anal. Calcd for $C_{11}H_{15}Br_2CuN_4O_2$: C, 28.81; H, 3.30; N, 12.22%. Found: C, 28.77; H, 4.11; N, 11.94%. Green needle crystals of **2** were prepared by using of $CuCl_2$ in place of $CuBr_2$. Anal. Calcd for $C_{11}H_{15}Cl_2CuN_4O_2$: C, 35.74; H, 4.09; N, 15.15%. Found: C, 36.19; H, 4.39; N, 14.79%.

X-ray diffraction data were collected on a Raxis-Rapid IP diffractometer (Rigaku) with graphite monochromated Mo Kα radiation (λ = 0.71073 Å) at 296 K. The crystal sizes were 0.2 × 0.1 × 0.1 and 0.2 × 0.03 × 0.03 mm^3 for **1** and **2**, respectively. Numerical absorption correction was applied. The structure was solved with the program SAPI-91[17] and refined using all the independent reflections with the program SHELXL-97.[18] Anisotropic temperature factors were used for non-hydrogen atoms. Significant peaks found in the channel on difference maps were assigned to water molecules with a small occupancy of 0.3. Selected crystallographic data of **1**·$(0.3H_2O)_6$ and **2**·$(0.3H_2O)_6$ are listed in Table 1.

Magnetic properties were measured on an MPMS SQUID magnetometer (Quantum Design) equipped with a 7 T superconducting magnet over a temperature range 1.8−300 K. Diamagnetic contribution of the sample itself was estimated from Pascal's constants.

Results and Discussion

Structural Studies. As Table 1 shows, the crystals of **1** and **2** are isomorphous, belonging to a space group trigonal $R\bar{3}$. We focus on the molecular and crystal structures of **1** here. Figure 1(a) shows a crystallographically independent unit for **1**, one $CuBr_2$·(4PMNN) moiety and a water molecule with an occupancy of almost 0.3, together with atom labeling. As Figure 1(b) shows, a molecule consists of a wheel-like hexamer of $CuBr_2$·(4PMNN) in a head-to-tail fashion, in which the pyrimidine (PM) rings work as μ-N1−C1−N2 bridges. The resultant hexagonal array shapes a cavity with a nanosized diameter; the interatomic distance of the opposing Cu1···Cu1* is 11.497(3) Å (the symmetry operation code for * is $-x, -y, -z$).

Selected bond lengths and angles of **1** and **2** are listed in Table 2. The molecular structure of **2** is quite similar to that of **1**, and the atoms of **2** are similarly numbered. The copper ion is pentacoordinated to form a square-pyramidal structure and is slightly deviated upward from the basal plane. Two bromide ions and two PM nitrogen atoms are bonded at the *trans*-equatorial positions. One oxygen atom in the nitronyl nitroxide (NN) group is coordinated at an axial position with the Cu−O distance of 2.216(6) Å for **1**, which is somewhat longer than

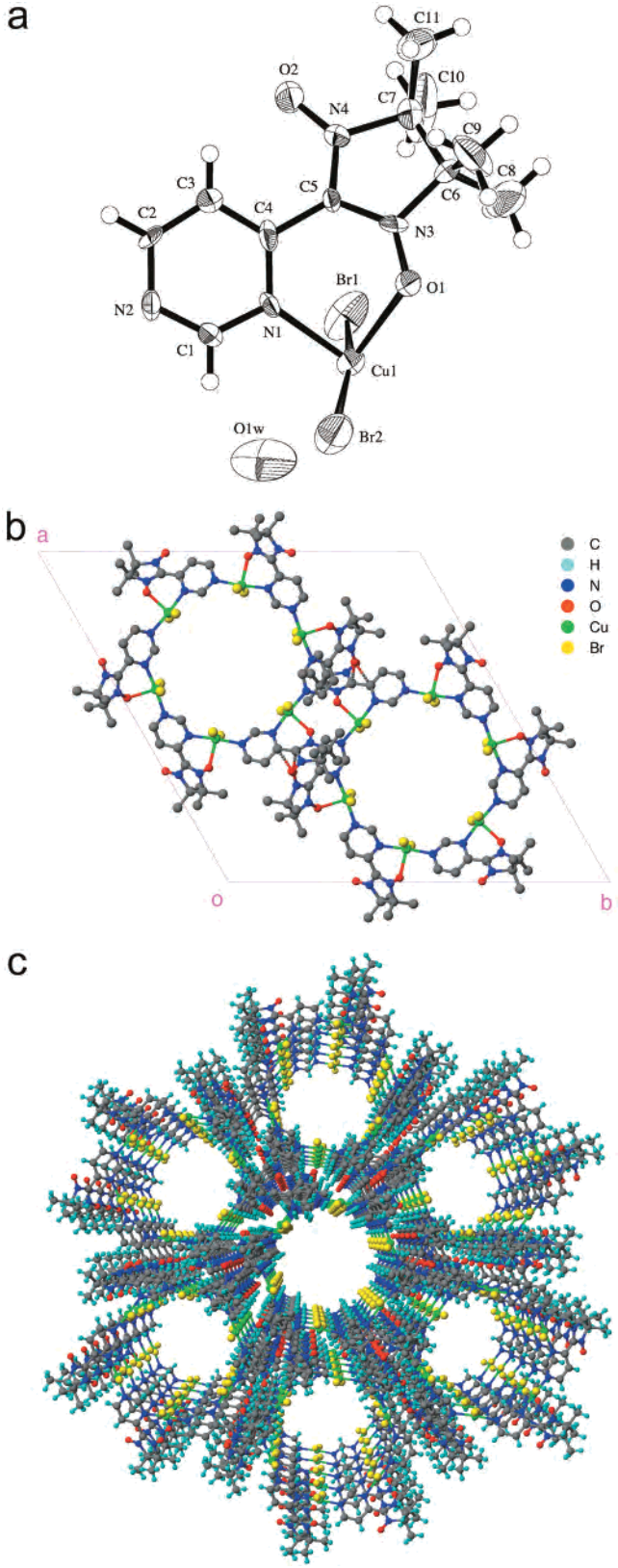

Figure 1. (a) Crystallographically independent unit of [$CuBr_2$·(4PMNN)]$_6$ (**1**) with atomic numbering. Thermal ellipsoids at the 50% level are shown for non-hydrogen atoms. Only oxygen atom (O1w) is shown for a water molecule with an occupancy of 0.3. (b) Two molecules of **1**. The hydrogen atoms and disordered water molecules are omitted. Intermolecular van der Waals contacts between O and C atoms are indicated with dotted lines. (c) Molecular arrangement in the crystal of **1** viewed along the *c* axis.

(17) Fan, H.-F. SAPI-91, Structure Analysis Program with Intelligent Control, Rigaku Corp., Tokyo, 1991.
(18) Sheldrick, G. M. Program for Crystal Structure Refinement, University of Göttingen, Germany, 1997.

Table 2. Selected Bond Lengths (Å) and Angles (Deg) of $[CuX_2 \cdot (4PMNN)]_6$ [X = Br (**1**), Cl (**2**)][a]

compound	**1**	**2**
Cu1 X1	2.3992(18)	2.249(2)
Cu1 X2	2.4010(18)	2.256(2)
Cu1 N1	2.020(7)	2.057(5)
Cu1 N2#	2.025(7)	2.030(5)
Cu1 O1	2.216(6)	2.262(4)
O1 N3	1.284(8)	1.286(6)
O2 N4	1.262(9)	1.269(6)
X1 Cu1 X2	162.39(7)	164.24(9)
N1 Cu1 N2#	175.6(3)	174.99(19)
N1 Cu1 O1	84.3(2)	83.38(16)
N2# Cu1 O1	91.4(3)	91.62(17)
O1 Cu1 X1	101.60(17)	100.86(13)
O1 Cu1 X2	95.97(17)	94.76(13)
N1 C4 C5 N3	−25.5(13)	−26.5(9)
O1 Cu1 N1 C1	−152.5(7)	−151.9(5)

[a] Symmetry code for #: $x - y, x, -z$.

the equatorial Cu1−N1 and Cu1−N2# distances (the symmetry code for # is $x - y, x, -z$). The C4−C5 bond between the two rings, PM and NN, is twisted by an angle of 26°, which is smaller than that of uncoordinated 4PMNN (44°).[19] The PM plane is largely canted from the Cu1 equatorial plane, as indicated by a dihedral angle between the PM ring and the axial Cu1−O1 bond. There are three molecules in a unit cell, and Figure 1(b) shows only two molecules in order to clarify intermolecular contacts between O2···C4§ and O2···C5§ (the symmetry code for § is $-y + 2/3, x - y + 1/3, z + 1/3$). Two contacts are drawn in Figure 1(b) with dotted lines. Each contact successively repeats, with a 3_1 screw symmetry along the *c* axis, and belongs to its individual magnetic chain. There are six chains running through a unit cell. Detailed intermolecular geometry of **1** and **2** will be discussed later.

As Figure 1(c) shows, the molecular hexanuclear arrays construct a column along the *c* axis, and consequently, a honeycomblike channel structure is formed. The intracolumnar neighboring molecular arrays are related by the translation along the *c* axis. No interatomic contact is found within a column, whereas intercolumnar atomic distances are relatively short. Note that the elemental analysis and X-ray diffraction study of **1** and **2** indicate that the channels are almost empty. Crystal solvents are supposed to be easily removed from the channel during usual evacuation process prior to the analysis.

Magnetic Properties. Figure 2 shows the temperature dependence of the product of magnetic susceptibility and temperature ($\chi_{mol}T$) for **1** and **2** measured at 500 Oe. The spin-only $\chi_{mol}T$ value of a molecule having twelve paramagnetic $S = 1/2$ spins is 4.5 cm^3 K mol^{-1}, assuming $g_{av} = 2.0$, being in apparent agreement with the experimental values. With decreasing temperature the $\chi_{mol}T$ values gradually decreased, but below ca. 40 K they turned to increase. Such a temperature dependence of $\chi_{mol}T$, showing a broad minimum, is often characterized for ferrimagnetic materials. However, **1** and **2** consist of two doublet species from copper(II) and an organic radical 4PMNN with a 1/1 molar ratio, and all of the copper(II) ions and radicals are crystallographically equivalent. Complexes **1** and **2** can hardly be regarded as ferrimagnetic materials. The "ferrimagnetic-like" behavior of **1** and **2** strongly suggests the simultaneous presence of ferro and antiferromagnetic interactions in their crystals.

With decreasing temperature below 40 K, the $\chi_{mol}T$ values increased and reached maxima of 35.6 and 22.6 cm^3 K mol^{-1} for **1** and **2**, respectively, and finally decreased again below ca. 3 K. The maximum values correspond to spin-only values of *S* of ca. 8 for **1** and *S* of slightly larger than 6 for **2**, suggesting that the ferromagnetic coupling should be attributed to interactions among the hexameric molecular arrays. The difference between the $\chi_{mol}T$ vs *T* profiles of **1** and **2** (Figure 2) do not seem to be intrinsic. Actually, the peak of the $\chi_{mol}T$ value was somewhat sample dependent. The magnetic properties may be changed in relation to the occupancy of the crystal solvent molecules included.

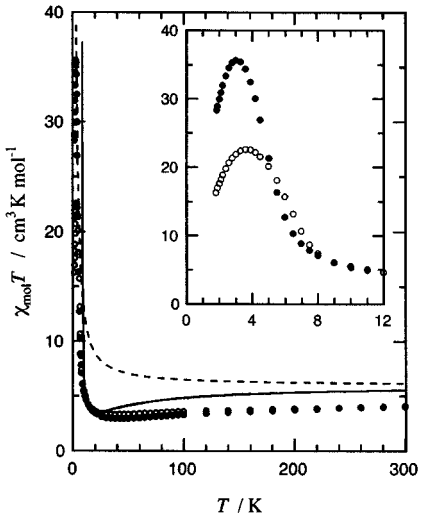

Figure 2. Temperature dependence of the product of χ_{mol} and *T* for $[CuX_2 \cdot (4PMNN)]_6$ [**1**: X = Br (filled circles), **2**: X = Cl (open circles)] measured at 500 Oe. Solid and Broken lines correspond to calculated curves based on a modified hexagonal model and the Fisher model, respectively. For the equations and parameters, see the text. Inset shows the magnification of the plot in a low-temperature region.

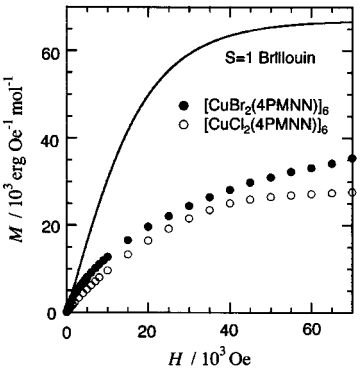

Figure 3. Magnetization curves of **1** and **2** measured at 2 K. The solid line represents a theoretical curve based on Brillouin function with $g_{av} = 2.0$ and $S = 1$.

The final decrease below ca. 3 K is more remarkable, and the maximum value is more suppressed in the measurements at larger applied fields. This finding indicates that the decrease is partly due to a saturation effect. To check whether antiferromagnetic phase transition occurs at around the peaking temperature, we measured the magnetization curves of **1** and **2** at 1.8 K (Figure 3). The magnetizations are very small and fall below the $S = 1$ Brillouin function with $g_{av} = 2.0$, clearly indicating the presence of dominant antiferromagnetic interaction. No inflection point was found in detailed d*M*/d*H* analysis in the *M*−*H* curves at 1.8 K. No anomaly was found in the measurements of field-cooled (5 Oe) or zero-field-cooled magnetization down to 1.8 K. Though **1** and **2** are paramagnets, the antiferromagnetic behavior is rationalized from the following discussion of the magnetic structure.

(19) Omata, J.; Ishida, T.; Hashizume, D.; Iwasaki, F.; Nogami, T. *Mol. Cryst. Liq. Cryst.*, in press.

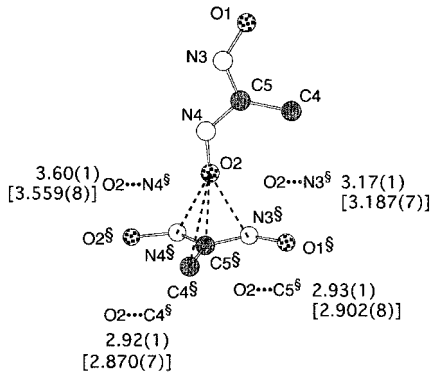

Figure 4. Intercolumnar atomic contacts for the crystal of **1** are shown in Å with dotted lines. Those values for the crystal of **2** are shown in square brackets. Only the ONCNO moiety and the C4 atom of the pyrimidinyl 4-position are drawn for the sake of clarity. The symmetry code for § is $-y + 2/3$, $x - y + 1/3$, $z + 1/3$.

Mechanisms of Magnetic Coupling. We can find a chelate structure in the repeating unit CuX_2·(4PMNN), in which the NN oxygen atom is axially coordinated to the copper ion. The orthogonality of Cu $3d_{x^2-y^2}$ and O $2p_z$ orbitals favors ferromagnetic interaction between the Cu and NN spins, as previously clarified for the one-dimensional Cu(II) complex bridged by methyl−NN.[1,20] The hexanuclear arrays are regarded as involving six local triplets at low temperatures.

On the other hand, we can also find that the PM bridges two copper ions. We have reported that the coordination structures of PM-bridged copper(II) complexes are simply classified into three types: axial−equatorial, equatorial−equatorial, and axial−axial coordinations of two nitrogen atoms in a PM ring.[9,10,21,22] The corresponding superexchange interactions are ferromagnetic, antiferromagnetic, and paramagnetic, respectively, through the PM ring.[9,10,21,22] In the present case, the PM bridge should be an antiferromagnetic coupler, since every PM nitrogen atom is coordinated at an equatorial position. Accordingly, the magnetism is expected to show antiferromagnetic coupling among six triplet units within a molecular array, and the experimental results above 40 K (Figure 2) agree with this interpretation. The increase of $\chi_{mol}T$ below 40 K must be attributed to intermolecular ferromagnetic interactions.

There is no interatomic contact within a column. As indicated with a dotted line in Figure 1(b), however, relatively short contacts can be pointed out between columns. Figure 4 shows selected atoms of adjacent 4PMNN groups. The shortest distance is found between a terminal NN oxygen atom and a carbon atom of the PM 4-position in a neighboring molecule. The O2···C4§ distances of 2.92(1) and 2.870(7) Å for **1** and **2**, respectively, are shorter than the sum of the van der Waals radii (3.2 Å).[23] The second shortest distance is found between a terminal NN oxygen atom and a central NN carbon atom (O2···C5§). Almost vertical spatial arrangement of two NN units forms a T-shaped configuration. We performed a semiempirical molecular orbital calculation of 4PMNN,[24] confirming that the NN group has a node of the singly occupied molecular orbital (SOMO) at the central carbon atom, and that none of the atoms of the PM group have appreciable coefficients of the SOMO. The O2···C5§ contact gives rise to ferromagnetic coupling on the basis of McConnell's theory.[25] Similar proximities were reported on ferromagnetic crystals of lithium *p*-NN-substituted benzoate[26,27] and 1,2,4-triazole-3-yl-NN,[28] and the ab initio calculation of exchange interaction demonstrated that such O···C(NN) contacts favored ferromagnetic interaction. Furthermore, Awaga has proposed that a large SOMO−NHOMO overlap due to contact between an NN group and an α-substituent (bonded to the central carbon atom) is required for appreciable ferromagnetic interaction.[29,30] Therefore, the first and second shortest contacts in the present complexes are both responsible for the observed ferromagnetic interaction. Figures 1b and 1c show that the intermolecular van der Waals contacts can be found to be surrounded by three columns, and this geometry successively repeats with a 3_1 screw symmetry along the *c* axis, forming a uniform linear chain. Along this interpretation, the crystals of **1** and **2** can be regarded as ferromagnetic chains accompanied by antiferromagnetic coupling among the chains.

Semiquantitative Analysis. To estimate semiquantitatively the exchange parameters (*J*'s),[31] J_{Cu-NN}, J_{Cu-Cu}, and J_{NN-NN} are defined between the copper(II) and axially coordinated NN spins, between two copper(II) spins across the PM ring, and between two NN spins through the van der Waals contacts, respectively. Below 40 K the ferromagnetic interaction was dominantly observed, which is due to the one-dimensional structure along the *c* axis with J_{NN-NN}. We applied the data of the $\chi_{mol}T$ upsurge region to the Curie−Weiss law, $\chi_{mol} = C/(T - \theta)$, to give positive Weiss temperatures; $\theta = 4.0$ and 3.8 K for **1** and **2**, respectively. The exchange parameters of several copper(II)−NN complexes in which the nitroxide oxygen is located in an axial site have been reported to possess $2J/k = 14-100$ K,[1] which is much larger than the θ obtained here. Actually, extrapolated values of $\chi_{mol}T$ at higher temperatures than 300 K seem to be larger than 4.5 cm^3 K mol^{-1}, indicating that J_{Cu-NN} is relatively large and positive (ferromagnetic). To simplify models, the Cu−NN unit is set to form a local triplet in a low-temperature region; i.e., $J_{Cu-NN} \gg J_{NN-NN}$ and $J_{Cu-NN} \gg |J_{Cu-Cu}|$. We adopt the following models to the present system. One is a hexagonal cluster model and the other a linear chain model. When the intramolecular interactions, J_{Cu-NN} and J_{Cu-Cu}, are predominantly opperative, rather than J_{NN-NN}, we choose a hexagonal cluster model.

Only the nearest-neighboring interaction is defined in a regular hexagonal arrangement of $S = 1$ sites. This model is expected to exhibit a monotonic increase or decrease in a $\chi_{mol}T$ versus *T* plot. Thus, we applied the van Vleck equation to this cluster model with modification of a Weiss mean field parameter θ', giving

$$\chi_{mol} = \frac{Ng^2\mu_B{}^2}{k(T-\theta')}\left[\frac{A}{B}\right]$$

with

$$A = 182 + 550\exp(12x) + 900\exp(22x) + 812\exp(30x) + 400\exp(36x) + 72\exp(40x)$$

$$B = 13 + 55\exp(12x) + 135\exp(22x) + 203\exp(30x) + 200\exp(36x) + 108\exp(40x) + 15\exp(42x)$$

(20) Caneschi, A.; Gatteschi, D.; Laugier, J.; Rey, P. *J. Am. Chem. Soc.* **1987**, *109*, 2191.
(21) Mohri, F.; Yoshizawa, K.; Yamabe, T.; Ishida, T.; Nogami, T. *Mol. Eng.* **1999**, *8*, 357.
(22) Yasui, M.; Ishikawa, Y.; Akiyama, N.; Ishida, T.; Nogami, T.; Iwasaki, F. *Acta Crystallogr., B* **2001**, *57*, 288.
(23) Bondi, A. *J. Phys. Chem.* **1964**, *68*, 441.
(24) Stewart, J. J. P. MOPAC version 6.0, *QCPE* #455. Stewart, J. J. P. *J. Comp. Chem.* **1989**, *10*, 209.
(25) McConnell, H. M. *J. Chem. Phys.* **1963**, *39*, 1910.
(26) Inoue, K.; Iwamura, H. *Chem. Phys. Lett.* **1995**, *207*, 551.

and

$$x = -J_{Cu-Cu}/kT$$

We estimated $J_{Cu-Cu}/k = -5$ K and $\theta' = +8.5$ K, and the calculated curve is superposed with a solid line in Figure 2. A broad minimum is reproduced, but upward deviation from the data is found in a high temperature region. This deviation is reasonably assigned to the disregard of thermal population of the Cu−NN singlets. The positive θ' value is related to ferromagnetic J_{NN-NN}.

To estimate J_{NN-NN}, the data are fit to the Fisher equation[32] for a uniform infinite chain of $S = 1$ classical spins

$$\chi_{mol} = \frac{Ng^2\mu_B{}^2S(S+1)}{3kT}\left[\frac{1+u}{1-u}\right]$$

$$u = \coth\left[\frac{2J_{NN-NN}S(S+1)}{kT}\right] - \left[\frac{kT}{2J_{NN-NN}S(S+1)}\right]$$

We obtained $J_{NN-NN}/k = +6$ K from the fit to the $\chi_{mol}T$ upsurge region, and the calculated curve is also shown with a dotted line in Figure 2. The larger discrepancy in a high-temperature region is due to the disregard of interchain antiferromagnetic interaction (J_{Cu-Cu}) and thermal population of the Cu−NN singlets. Although in this treatment J_{NN-NN} is probably underestimated because the antiferromagnetic interaction is not excluded from the data, the obtained J_{NN-NN} is roughly compatible with the positive θ' obtained by the analysis on the hexagonal model.

The magnetic behavior of the present complexes is rationalized by the competitive magnitudes of J_{NN-NN} and $|J_{Cu-Cu}|$. The final decrease of the $\chi_{mol}T$ values is explained as follows. The hexagonal molecule has a ground singlet state due to the negative J_{Cu-Cu}. The crystal becomes antiferromagnetic despite the presence of intermolecular ferromagnetic interaction. Even when the ferromagnetic correlation preferentially grows along the column, the triplet Cu−NN spin pairs are arranged completely in alternate rows in a hexagonal lattice, and consequently the antiferromagnetic behavior was observed as an indication of a possible antiferromagnetic order below 1.8 K.

Concluding Remarks

Discrete hexanuclear complexes **1** and **2** construct a perfect column perpendicular to the macrocyclic molecular plane. The ferromagnetic couplings observed are attributed to the interactions between a copper spin and the axially coordinated nitronyl nitroxide spin and also between nitronyl nitroxide groups through the van der Waals contacts. The diameters of the honeycomblike channel structures are ca. 11.5 Å, and they form ferromagnetic one-dimensional structures in the column direction. Thus, we can think of these complexes as "magnetic nanotubes". We have attempted the synthesis of host−guest complexes of **1** and **2**, because the inner vacant axial sites are available for further coordination, and found that the magnetic properties changed depending on guest molecules. Details will be reported separately.

Acknowledgment. This work was supported by Grants-in-Aid for Scientific Research on Priority Areas of "Molecular Conductors and Magnets" (No. 730/11224204) and "Creation of Delocalized Electronic Systems" (No. 297/12020219) from the Ministry of Education, Science, Sports and Culture, Japan.

Supporting Information Available: Crystallographic data (excluding structure factors) for the structures of **1**·$(0.3H_2O)_6$ and **2**·$(0.3H_2O)_6$, in CIF format. This material is available free of charge via the Internet at http://pubs.acs.org.

IC001462G

(27) Kawakami, T.; Oda, A.; Mori, W.; Yamaguchi, K.; Inoue, K.; Iwamura, H. *Mol. Cryst. Liq. Cryst.* **1996**, *279*, 29.
(28) Kawakami, T.; Yamaguchi, K.; Matsuoka, F.; Yamashita, Y.; Kahn, O. *Polyhedron*, in press.
(29) Awaga, K.; Inabe, T.; Maruyama, Y. *Chem. Phys. Lett.* **1992**, *190*, 349.
(30) Awaga, K. In *Magnetic Properties of Organic Materials*; Lahti, P. M., Ed.; Marcel Decker: New York, 1999; Chapter 25, pp 519−534.
(31) The exchange parameter J between two spins S_i and S_j is defined by the spin Hamiltonian $H = -2J\,S_i \cdot S_j$.
(32) Fisher, M. E. *Am. J. Phys.* **1964**, *32*, 343.